TISSUE ENGINEERING: Part A
Volume 19, Numbers 3 and 4, 2013

DOI: 10.1089/ten.tea.2012.0382

The Development of a ε-Polycaprolactone Scaffold for Central Nervous System Repair

Peter S. Donoghue, BSc, PhD,[1] Rebecca Lamond, BSc,[1] Stephanie D. Boomkamp, BSc, PhD,[1]
Tao Sun, BSc, PhD,[2,3] Nikolaj Gadegaard, BSc, MSc, PhD,[4]
Mathis O. Riehle, BSc, PhD,[2] and Susan C. Barnett, BSc, PhD[1]

Potential treatment strategies for the repair of spinal cord injury (SCI) currently favor a combinatorial approach incorporating several factors, including exogenous cell transplantation and biocompatible scaffolds. The use of scaffolds for bridging the gap at the injury site is very appealing although there has been little investigation into the central nervous system neural cell interaction and survival on such scaffolds before implantation. Previously, we demonstrated that aligned microgrooves 12.5–25 μm wide on ε-polycaprolactone (PCL) promoted aligned neurite orientation and supported myelination. In this study, we identify the appropriate substrate and its topographical features required for the design of a three-dimensional scaffold intended for transplantation in SCI. Using an established myelinating culture system of dissociated spinal cord cells, recapitulating many of the features of the intact spinal cord, we demonstrate that astrocytes plated on the topography secrete soluble factors(s) that delay oligodendrocyte differentiation, but do not prevent myelination. However, as myelination does occur after a further 10–12 days in culture, this does not prevent the use of PCL as a scaffold material as part of a combined strategy for the repair of SCI.

Introduction

The intrinsic inability of central nervous system (CNS) neurons to regenerate, coupled with the formation of a gliotic scar are the major contributing factors to the irreparable nature of spinal cord injury (SCI).[1,2] As a consequence, numerous treatment strategies have been considered including, exogenous cell transplantation and disruption of the glial scar by biological and pharmacological agents, with limited success. Moreover, after cell transplantation, even with extensive in-growth, axonal orientation is often random within the lesion, with few axons exiting the graft and entering the distal host tissue.[1,3,4] To overcome these specific problems, implantation of biocompatible oriented scaffolds of biodegradable polymers has been designed to promote aligned axonal outgrowth across the lesion.[5–9]

Numerous potential substrates have been investigated for use in scaffold design, including (1) biocompatible hard degradable polymers, for example, ε-polycaprolactone (PCL),[10] poly-L-lactide (PLLA),[11] poly(lactic-*co*-glycolic acid) (PLGA), and chitosan, or (2) hydrogels both naturally occurring, for example, agarose[12] and collagen, or synthetic, each possessing unique properties and characteristics. Polymers can also be blended with each other, to combine properties of their constituent materials including PCL/PGLA[13] and PCL/chitosan.[14,15] They can be combined with other treatment strategies, such as cell transplants including glia that is, Schwann cells or olfactory ensheathing cells (OECs), neural progenitor cells, or stem cells[16–19]; or impregnated with compounds noted for their neurotrophic properties or ability to disrupt the inhibitory scar environment. This combinatorial approach has demonstrated some success in the encouragement of neurite outgrowth or functional recovery, such as the combination of a PCL scaffold with neural progenitor cell implantation and perfusion with chondroitinase ABC,[18] or PCL nanofibers impregnated with the brain-derived neurotrophic factor.[20]

Previously, our group has reported that the inclusion of microgrooves on a PCL substrate promotes the aligned growth of axons within a CNS culture[21] and can be incorportated into a three-dimensional (3D) Swiss roll style scaffold by rolling up a porous, patterned PCL sheet.[22] The pores enable mass transfer within the 3D scaffold and previous work has demonstrated that a pore diameter of at least 200 μm prevents occlusion by astrocytes.[22,23] This 3D scaffold will eventually be coated with glial cells, as part of a

[1]Institute of Infection, Immunity and Inflammation, College of Medical, Veterinary and Life Sciences, University of Glasgow, Glasgow, United Kingdom.
[2]Centre for Cell Engineering, Institute of Molecular, Cell and Systems Biology, College of Medical, Veterinary and Life Sciences, University of Glasgow, Glasgow, United Kingdom.
[3]Department of Biological Sciences, Xi'an JiaoTong-Liverpool University, People's Republic China.
[4]Biomedical Engineering, School of Engineering, University of Glasgow, Glasgow, United Kingdom.

combinatorial approach to treat SCI, to promote the ingrowth of endogenous CNS cells in an aligned manner to aid crossing the graft. Before the implantation of this complicated 3D Swiss roll, we have adopted a systematic approach to investigate the different features of the scaffold design to fully assess their potential effects on CNS cells using dissociated rat spinal cord cells. These cells interact to mimic the complex cellular interactions of CNS cells *in vivo*.[24–26] Although many studies have primarily investigated biocompatibility, cytotoxicity, and the immune response following implantation,[27] we have focused on how the host CNS cells, including astrocytes, neurons, microglia, and their myelinating glia respond to the scaffold design with emphasis on differentiation as a read out, which indicates the potential effectiveness of the scaffold to support repair in the CNS.

Materials and Methods

Cell seeding

Preparation of the striatal neurosphere-derived astrocytes. Myelinating CNS cultures were set up as previously outlined,[24,25] with a couple of minor modifications. They comprise a monolayer of astrocytes on top of which are plated mixed rat spinal cord cells. Astrocytes are essential for cell survival and myelination.[24] Briefly, striatum were collected from P1 Sprague-Dawley rats in Liebowitz (L15; Invitrogen) media and dissociated mechanically before suspension in neurosphere media (Dulbecco's modified Eagle's medium, DMEM/F12 (1:1), 0.6% glucose, 2 mM glutamine (Invitrogen), insulin (25 mg/mL; Sigma), 5 mM Hepes (Sigma), 0.105% $NaHCO_3$ (Sigma), 5000 IU/mL penicillin (Invitrogen), 5 mg/mL streptomycin (Invitrogen), 100 mg/mL apotransferrin, 20 nM progesterone, 60 mM putrescine, and 30 nM sodium selenite (all Sigma) supplemented with 20 ng/mL mouse submaxillary gland epidermal growth factor (EGF; R&D systems) and cultured as neurospheres for 7–10 days at 37°C, 7% CO_2, with supplementation of the media every alternate day.

Neurospheres were differentiated into astrocytes in a T150-cm^2 flask using the low-glucose DMEM (Invitrogen) containing 10% fetal bovine serum (referred to as 10% FBS) for 7–8 days. Since astrocytes derived from neurospheres or the cortex support myelination in these cultures, we used neurosphere-derived astrocytes as they more rapidly generate many purified cells.[24,25] Differentiating astrocytes in a flask before seeding enabled the calculation of defined cell numbers sufficient to form a confluent monolayer after seeding onto a glass coverslip or polymer substrate. This compensated for any difficulties assessing if the monolayer was confluent due to the opacity of the polymers. Astrocytes were passaged with trypsin/EDTA (0.25%, Invitrogen) and plated onto either poly-l-lysine (PLL, Sigma, 13 μg/mL)-treated glass coverslips (VWR International) or a polymer substrate at a density of 200,000 cells per 100 μL. The astrocytes were maintained in 10% FBS.

Preparation of the myelinating cultures. The spinal cord from E15 Sprague-Dawley rat embryos were dissected, the meninges removed, chopped, and digested in trypsin and collagenase for 15 min followed by enzymatic inhibition with a soybean trypsin inhibitor (0.52 mg/mL), bovine serum albumin (3.0 mg/mL), and DNase (0.04 mg/mL; all Sigma). The cell suspension was centrifuged at 12,000 rpm for 5 min, resuspended in plating media (DMEM 21885, containing 20% horse serum, HBSS, L-glutamine), plated onto astrocyte monolayers at 150,000 cells per 100 μL and left for 2 h at 37°C, 7% CO_2 before feeding with a mix of plating media and differentiation media (DMEM 196966, Invitrogen, 50 nM hydrocortisone, 10 ng/mL biotin, 4 μM progesterone, 20 mM putrescine, 6 μM selenium, 1 m/mL apotransferrin, supplemented with 10 μg/mL insulin (all Sigma). The cultures were maintained with fresh differentiation media on alternate feeding days, with the insulin supplement removed from 12 days *in vitro* (DIV).

Construct preparation

Preparation of polymer-coated coverslips for materials testing. Several polymers were used in testing compatibility with survival and differentiation of the myelinating cultures, including PCL (high molecular weight: 90,000 and low molecular weight: 45,000, both Sigma); Polycarbonate (PCB, Bayer Makrolon OD2015); Polystyrene (PS, Proprietary grade); PLLA (Ingeo™ Biopolymer D3001, Nature Works LLC); Poly(methyl) methacrylate (PMMA; Evonik Degussa Plexiglas® 6N). All were dissolved in chloroform at 10% (w/v), and used for spin-coating coverslips. Glass coverslips (13 mm diameter) were placed in a spin coater and 150 μL of polymer solution applied before spinning at 2000 rpm for 15 s, with 200 rpm/s acceleration and 200 rpm/s deceleration. Polydimethylsiloxane (PDMS; Dow Corning) was prepared by mixing Sylgard 184 at a ratio 10:1 of base and curing agent, degassed for 20 min, and cast against a fluorinated silicon wafer to achieve a flat substrate.

Preparation of the PCL membrane. The PCL membranes were prepared by washing PCL pellets (MW: 45,000 or 90,000; Sigma) with methanol, with subsequent drying and dissolution into chloroform, (15% w/v, concentration) overnight on a shaker platform. The PCL/chloroform solution was then applied to a silicon wafer either with a flat surface, or, for a porous PCL membrane, with equidistant cylindrical pillars across its surface. Once the PCL solution was applied to the wafer, it was spin coated at 1000 rpm for 30 s, ramp 200 rpm/s, and the chloroform allowed to evaporate in sterile air. The resultant PCL membrane, which was ~20 μm thick, was then wetted with 70% ethanol before removing from the wafer to avoid disruption of membrane integrity.

The microgrooved topography was applied using the hot embossing protocol previously described.[20] Briefly, the PCL membrane was sandwiched between an unpatterned PDMS mask and a PDMS mask with an aligned micropattern. Once cooled, the patterned PCL membrane could be used in further construct preparation, with 0.5-cm × 1-cm sections being cut and attached to a support scaffold, as required for their appropriate maintenance in culture. The support scaffold was constructed using 4 polycarbonate struts arranged in two parallel rows, with one row resting on the other forming a square and the struts were stuck together using molten PCL. The PCL membrane could then be attached spanning between parallel rows, leaving a 0.6-cm × 0.5-cm area for cell seeding. The scaffolds were placed on a coverslip for cell seeding as a meniscus in 100 μL (as with the glass coverslips), and transferred to a larger polycarbonate scaffold to keep the

membrane suspended. The fabrication scheme is summarized in Figure 1. Unpatterned membranes were used to assess if the micropattern and/or PCL affected differentiation within the myelinating cultures.

Preparation of the polymers for cell culture. In all experiments, the hydrophobicity of the polymers was reduced with air plasma using a Harrick Plasma Cleaner (Harrick Plasma) at Hi settings (740 V DC, 40 mA DC, 29.6 W) for 5 min before the application of PLL and use in cell culture.

Immunocytochemistry

For intracellular markers, cells were fixed in 4% paraformaldehyde and permeabilized with phosphate-buffered saline containing 0.2% (w/v) gelatin and 0.1% (v/v) Triton X-100™. Cell surface markers (i.e., the O4 antibody, A2B5, and the chondroitin sulfate proteoglycan NG2) were applied to live cells, followed by Alexa Fluor anti-mouse IgM or anti-rabbit secondary (Cambridge Biosciences), before methanol fixation. The primary antibodies used were SMI-31 (1:1,500, mouse monoclonal IgG1, Abcam, labels phosphorylated neurofilament), AA3, raised against the proteolipid protein (PLP-DM20, 1:100, anti-rat) and defines mature myelin,[28] the astrocytic marker, the glial fibrillary acidic protein (GFAP, 1:100, rabbit polyclonal; DAKO), O4 (1:1, hybridoma, IgM, oligodendrocyte marker), and A2B5, (1:1, hybridoma, IgM, oligodendrocyte precursor cell (OPC) marker) both gifts from Mark Noble[29] and NG2 (1:100, rabbit polyclonal, Chemicon, early OPC). The secondary antibodies were from the Alexa Fluor range (1:100; Invitrogen). Nuclei were visualized using DAPI included in the hard set mountant (Fluoro-Gel; Interchim).

Imaging

Images were captured using an Olympus BX51 microscope with Q imaging software Images and analyzed using Image Pro Plus (Media Cybernetics).

Quantification and statistics

Quantification of myelination. To quantify myelination as defined by the percentage of fibers ensheathed by a myelin sheath, the cultures were labeled with SMI-31 (green), anti-PLP myelin (red), and DAPI (blue). Ten images per coverslip were acquired at ×10 magnification as previously described[23] and initially opened using ImageJ with the blue (DAPI) channel removed. The red and green images were then opened with Adobe Photoshop Elements 7.0 and areas of myelin that was a clear sheath were overlaid by hand using a brush tool in blue in a new, lightened layer. The percentage of myelination was calculated using ImageJ by taking the neurite density, (as recorded by the red pixels), and calculating the percentage of neurites ensheathed by myelin (blue area in pixels). The calculations were produced using our own macro in ImageJ. For comparison of values between groups of conditions, data were analyzed by calculating ratios and analyzing these with one-sample Student's t tests, using 1 as the null hypothesis mean. The mean of a minimum of 3 experiments per condition in duplicate was used, and all values are expressed as means ± SEM. Significance was represented using p-values, where values ± 0.05 were considered significant for comparisons using only two samples, and are indicated by an asterisk on images. A Bonferroni correction was applied when there were multiple samples being compared with the control, with a lower p-value being used to determine significance.

Analysis of cell differentiation. Images of the myelinating cultures labeled with oligodendrocyte lineage markers: anti-NG2, the A2B5, and O4 antibody were opened using ImageJ and the channels split, with each cell labeled being identified and calculated as a percentage of the total number of DAPI-stained nuclei. O4 expression differed in that the extensive arborisation of the O4-positive cells made identifying individual cells difficult, so the percentage coverage by O4-positive processes was calculated and divided by the total

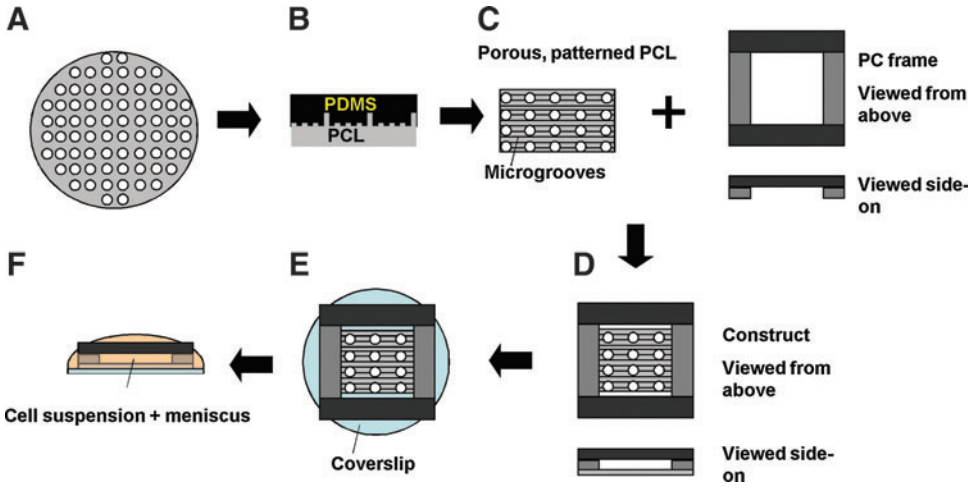

FIG. 1. Schematic for construct preparation. The porous ε-polycaprolactone (PCL) membrane is prepared by spin-coating **(A)** and subsequently hot-embossed with an aligned micropattern using a polydimethylsiloxane (PDMS) stamp **(B)**. The resultant porous, micropatterned PCL membrane is then fixed to a polycarbonate scaffold **(C, D)** and mounted on a 13-mm glass coverslip **(E)** for seeding with the appropriate cell type **(F)**, which sit in a meniscus as with a control coverslip. The coverslip was subsequently removed after the cells had settled and the construct suspended on a larger polycarbonate scaffold. Color images available online at www.liebertpub.com/tea

cell number as indicated by DAPI staining. All experiments were conducted in duplicate with at least 3–5 separate experiments.

Results

The percentage of myelination was greater in cultures plated on PCL compared to other substrates

To determine which material would be most suitable for transplantation into the CNS and be supportive of endogenous neural cell survival and differentiation, we studied their ability to support myelination in mixed spinal cord cell cultures. In general, the maximum percentage of myelination in the cultures ranges from 2%–10% after 28 DIV as many of the fibers generated in culture are interneurons. Previously, we have demonstrated that myelin is compacted[25] and formed correctly with the correct location of nodal proteins in these cultures.[24] Comparisons were made to a positive control of cultures grown on a PLL-coated glass coverslip (to assure us that the cultures are differentiating correctly), and the following PLL-coated test substrates: PCL (low (L) and high (H) Mw), PC, PMMA, PS, PLLA, and PDMS (Fig. 2). Previous work has demonstrated the usefulness of this control in comparing the ability of several reactive astrocyte phenotypes in supporting myelination.[30]

The neurite density (SMI-31 immunoreactivity) on the polymer substrates was comparable to that of control glass coverslips, an important indicator of neuronal survival and process extension, but myelination was significantly lower ($n=3$, t-test, Bonferroni corrected, $^*p<0.05$) on all polymer substrates when compared to the control. The lower molecular weight PCL supported the highest level of myelination of all the polymers, but was not suitable for further use, being too fragile to survive the hot embossing and subsequent 3D manipulations intact. Expansion of the culture time beyond 28 days on these various substrates resulted in nonviable cultures and could not be analyzed (suggesting lack of compatability for long-term cultures) except for the two PCL substrates. The high molecular weight PCL was considered the optimal substrate.

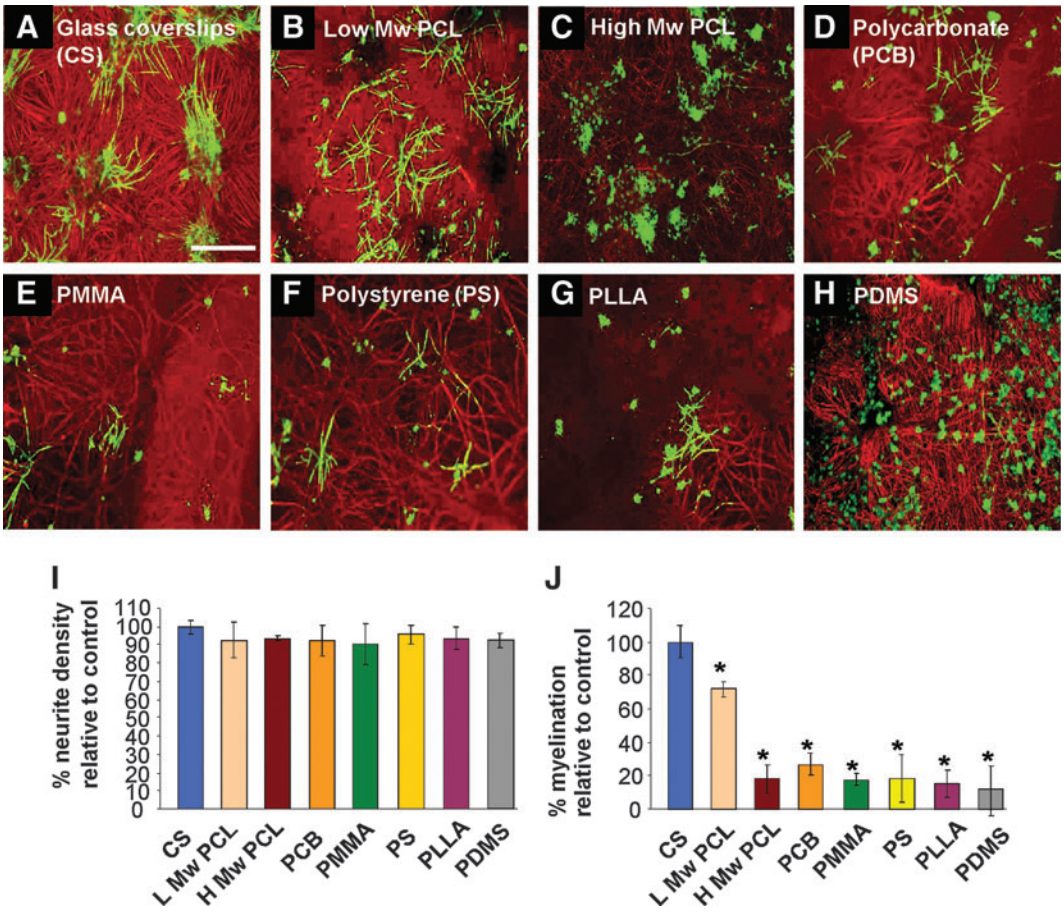

FIG. 2. PCL is the most suitable polymer for supporting myelination in mixed neural cell cultures. Representative images of a myelinating culture after 28 days *in vitro* (DIV) and stained for SMI-31 (red, neurons) and proteolipid protein (PLP, green, myelin), plated onto either glass coverslips **(A)**, low molecular weight PCL **(B)**, high molecular weight PCL **(C)**, polycarbonate **(D)**, poly(methyl) methacrylate (PMMA) **(E)**, polystyrene (PS; **F)**, poly-L-lactide (PLLA) **(G)**, or polydimethylsiloxane (PDMS) **(H)**. Scale bar: 100 μm. Quantitative analysis of neurite density **(I**; SMI-31 immunoreactivity in a given area**)** and myelination **(J**; measured by the percentage of neurite density occupied by myelin ensheathed axons in a given area**)** show little change in the percentage of neurite density on each of the polymers, but significant decrease in myelination compared with the glass coverslips **(J**; $n=3$, t-test, Bonferroni corrected, $^*p<0.05$**)**, with PCL supporting the greatest level of myelination among the polymers. Color images available online at www.liebertpub.com/tea

Myelination is decreased on PCL substrates compared to control

To investigate if the topological discontinuities the micropattern, the pores, and the combined micropattern and pores in the PCL membrane[21,31] would affect CNS cell survival and myelination, we compared cell biological properties between CNS cultures on the PLL-coated flat PCL membrane (Fig. 3B), the porous PCL membrane (Fig. 3C), and the porous PCL membrane possessing an aligned micropattern as substrates (Fig. 3D). After 28 DIV, myelination was an average of 5% on the control glass coverslips, whereas it was reduced to 2% when the cells were plated on each of the PCL substrates (Fig. 3E this was a significant reduction in myelination $n=3$, t-test, Bonferroni corrected, $^*p<0.05$) compared to control glass coverslips. Neither the topography nor the presence of pores reduced the neurite density (Fig. 3F), or prevented the outgrowth of processes despite a reduction in myelination at this time. To test if potential contaminants leaching from the PCL into the culture environment affected myelination, cultures on glass were incubated with PCL beads throughout. After 28 DIV, neither the neurite density ($80.2\% \pm 0.3\%$ for the control compared to $79.8\% \pm 0.4\%$ in the presence of PCL beads), nor myelination was affected ($4.0\% \pm 0.5\%$ for control, $3.7\% \pm 0.3\%$ in the presence of PCL beads). This suggests that factors leached from PCL did not affect myelination.

Surface treatment of the PCL substrate fails to enhance myelination

In an attempt to investigate whether extracellular matrix (ECM) coatings would enhance myelination PCL, substrates were coated with collagen (Fig. 4B), fibronectin (Fig. 4C), and laminin (Fig. 4D), subsequent to plasma activation, but before cell seeding with the myelinating cultures (and astrocytes monolayer). These ECM proteins have been shown to enhance myelination when in direct contact with neurons plated on glass coverslips.[32,33] PLL-coated PCl substrates were used for comparison (Fig. 4E). After 28 days, the cultures were immunolabeled with antibodies to SMI-31 (red) and PLP (green) and myelination quantified. Each of the surface treatments were detrimental to the survival and differentiation of the cultures, with the neurite density significantly decreased in the myelinating cultures plated on laminin- treated PCL (Fig. 4F; $n=3$, t-test, Bonferroni corrected, $^*p<0.05$), suggesting that neurons did not survive well nor extend as many neurites as seen on the control substrate. The levels of myelination on all ECM-treated substrates were significantly reduced compared to both glass coverslips treated with PLL and PCL treated with PLL (Fig. 4G; $n=3$, t-test, $^*p<0.05$). This suggests ECM treatment of the PCL induces a change in the astrocyte monolayer making it less supportive of myelination. A similar reduction in myelination has been reported when astrocytes were plated on the ECM molecule tenascin C.[30]

Oligodendrocyte differentiation on PCL is altered compared to glass

To investigate if the the PCL substrate affected oligodendrocyte differentiation stages, cultures were immunolabeled at 7 and 14 DIV for three oligodendrocyte lineage-specific markers. These include the OPC markers, NG2 (Fig. 5A–D), and A2B5 (Fig. 5E–H), and the immature oligodendrocyte

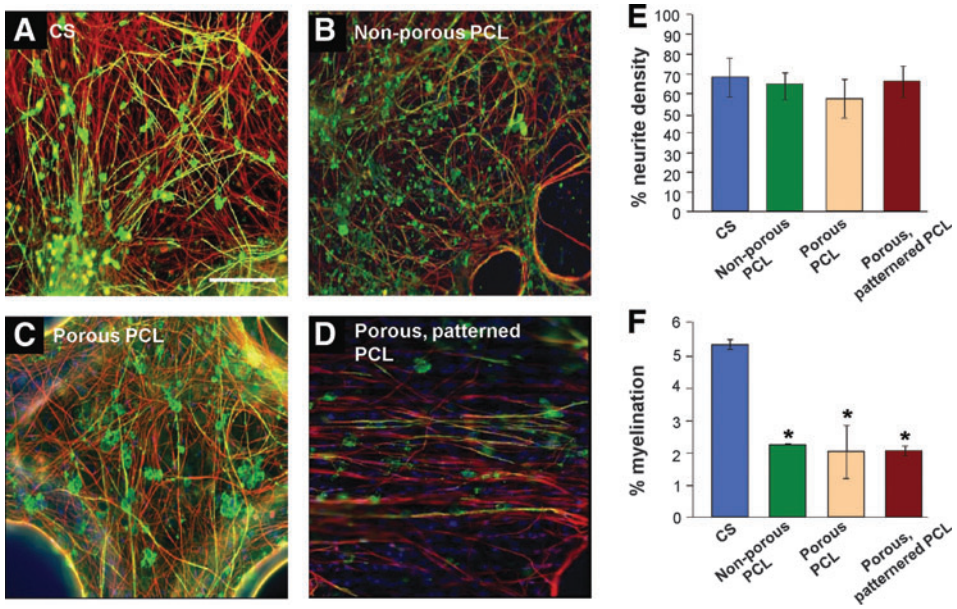

FIG. 3. Myelination is less when myelinating cultures are plated on PCL compared to glass coverslips and stained after 28 DIV. Representative images of myelinating cultures on different substrates immunolabeled for SMI-31 (red) and PLP (green) after 28 DIV. Nuclei were visualized with DAPI. Control cultures on glass coverslips **(A)** show extensive neurite coverage, which were ensheathed with myelin, whereas cultures plated on the nonporous PCL **(B)**, porous PCL **(C)**, and porous, micropatterned PCL **(D)** contained similar neurite density, but less myelination. Quantification of both myelination **(E)** and neurite density **(F)**, respectively, for each of the PCL substrates showed a significant decrease in myelination compared to the glass **(F**; $n=3$, t-test, Bonferroni corrected, $^*p<0.05$**)**. Scale bar: 100 μm. Color images available online at www.liebertpub.com/tea

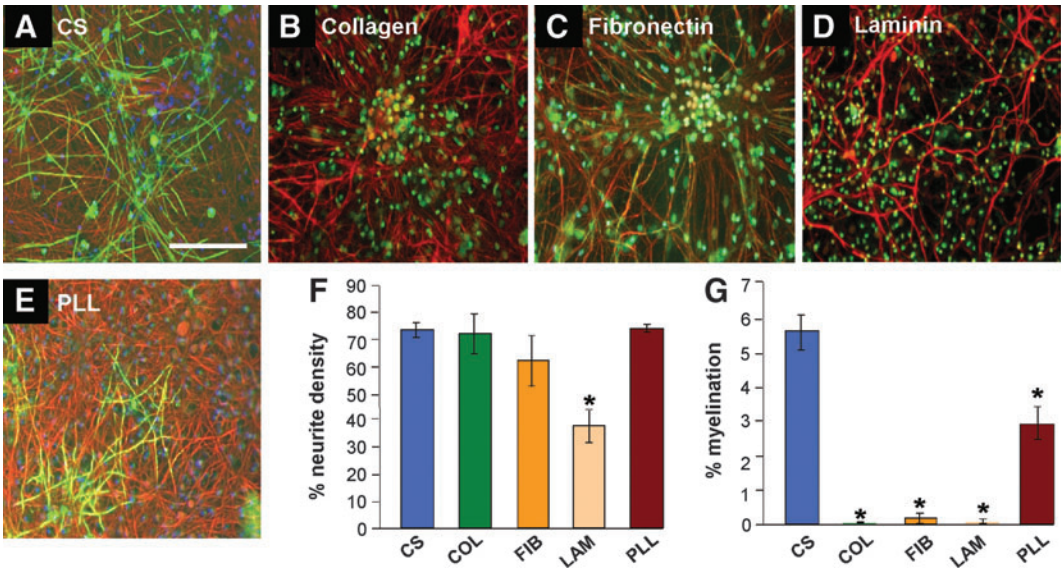

FIG. 4. Surface treatments fail to enhance myelination on PCL. Representative images of myelinating cultures plated onto either glass coverslips **(A)** or PCL coated with collagen **(B)**; fibronectin **(C)** and laminin **(D)**, or poly-l-lysine (PLL) alone **(E)**. Quantification of neurite density for the cultures on each substrate shows that, with the exception of the cultures plated on laminin, neurite density was comparable to the glass coverslips **(F)**. Quantification of the percentage of myelination **(G)** showed a significant decrease compared to both the glass coverslip and PCL treated with PLL only ($n=3$, t-test, Bonferroni corrected, $^*p<0.05$). Scale bar: 100 μm. Color images available online at www.liebertpub.com/tea

marker, O4 (Fig. 5I–L). The myelinating cultures plated onto PCL had a higher percentage of immature A2B5-positive (+), and NG2-positive (+) oligodendrocyte lineage cells at both 7 DIV and 14 DIV compared to cells plated on glass coverslips. However, the NG2+ cells had a less branched morphology, indicative of a more immature phenotype, than those plated on coverslips, which was especially apparent by 14 DIV. The density of O4 immunoreactivity also covered a greater area on the PCL compared to cultures plated onto glass coverslips, suggesting either a greater number of O4+ cells, or more extensive arborisation. As the cell density was so high, it was difficult to accurately count individual cells; so, values for O4 immunoreactivity was divided by DAPI-positive nuclei. At day 21, expression of the mature myelin marker, PLP, demonstrated that oligodendrocytes in the myelinating cultures on the glass coverslips had already begun to myelinate, with detectable sheaths forming (Fig. 5M), while on the PCL, the oligodendrocyte morphology was consistent with a premyelinating phenotype, morphologically similar to the O4+ cells observed at earlier time points on glass. Taken together, this data suggests that there is a delay in the maturation of oligodendrocytes in the myelinating cultures plated onto PCL, with a larger proportion of immature and premyelinating oligodendrocytes present (Fig. 5N bar charts).

Myelination on PCL substrate is delayed compared to cultures plated on glass coverslips

To assess if the greater number of immature oligodendrocytes in the cultures plated on PCL (Fig. 5) after 28 DIV and the delay in myelination was a timing issue, we extended the culture period to 46 DIV. (Fig. 6). With the exception of the nonporous PCL (Fig. 6B), myelination on the PCL substrates after 46 days was comparable (t-test, $n=3$, Bonferroni corrected, $^*p<0.05$) to cultures on glass coverslips (Fig. 6A), suggesting that oligodendrocyte differentiation is delayed, and not inhibited on PCL. The neurite density for each of the conditions was comparable with no obvious signs of culture deterioration on any substrate. With the micropatterned porous PCL being the final design for the rolled 3D scaffold, this was the substrate used for further investigation.

The astrocyte substrate can influence myelination

Our previous data suggested that the reactive status/phenotype of astrocytes and the subsequent changes in factors secreted by these can affect myelination.[24,30] To examine if the substrate influence on myelination was mediated via astrocyte secreted factors, we included a monolayer of astrocytes plated either onto glass coverslips (cond. CS, Fig. 7D) or onto PCL substrates (cond. PCL, Fig. 7B) in the Petri dish containing myelinating cultures plated PCL substrates or glass coverslips, respectively. After 28 DIV, the myelinating cultures plated on glass coverslips, conditioned by coculture with astrocytes plated on PCL (Fig. 7B; labeled with the SMI-31 antibody (red) and anti-PLP (green)) had significantly less myelination compared to control cultures plated on glass (Fig. 7A). This indicates that astrocytes plated on PCL produce, and release (a) secreted factor(s) that contribute to a delay in myelination independent of direct cell contact. Interestingly, the myelinating cultures plated on astrocytes on PCL cocultured with a monolayer of astrocytes plated on glass coverslips (Fig. 7D) had levels of myelination comparable to cultures plated on glass coverslips (Fig. 7A; t-test, $n=3$, Bonferroni corrected, $^*p<0.05$) suggesting the delay in myelination on the PCL substrate can be overcome by promyelinating factors secreted by astrocytes, which were cultured on glass.

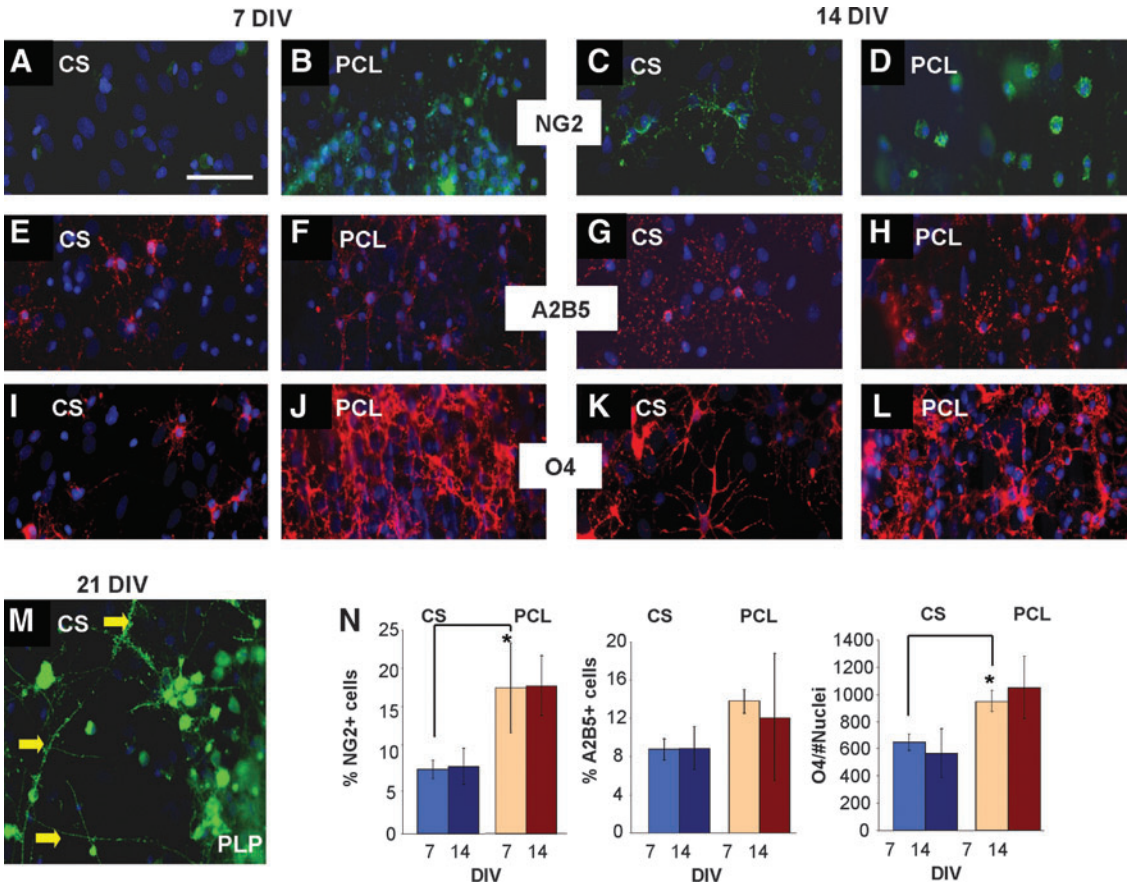

FIG. 5. Oligodendrocyte differentiation on PCL membranes is altered compared to glass coverslips. Representative images of myelinating cultures plated onto coverslips **(A, C, E, G, I, K, M)** or PCL **(B, D, F, H, J, L, N)** immunolabeled for NG2 **(A–D)**, A2B5 **(E–H)**, or O4 **(I–L)**, markers of increasing oligodendroglial maturity at both 7 DIV and 14 DIV, with the percentage of A2B5+ cells and NG2+ cells calculated from a total cell number as indicated by DAPI (blue) staining. The total coverage of O4+ processes was also calculated and divided by the total DAPI count to give a ratio of O4+ coverage to total cell number. At 7 DIV, a significantly higher percentage of NG2+ cells ($n=3$, t-test, $^*p<0.05$), were observed on the PCL compared with the coverslips, with this trend detectable at both 7 DIV and 14 DIV with regard to the percentage of A2B5+ cells and O4+ coverage (significant for 7 DIV, when myelinating cultures on PCL were compared with coverslips, $n=3$, t-test, $^*p<0.05$), suggesting a greater number of oligodendrocytes on the PCL. At 21 DIV **(M)**, the morphology of the oligodendrocytes detectable with PLP immunolabeling, indicated the presence of what were likely to be myelin sheaths (yellow arrows) in the cultures on the coverslips, whereas those on the PCL still possessed an immature morphology. Scale bar: 100 μm. Color images available online at www.liebertpub.com/tea

Discussion

The ability of CNS cells to survive and differentiate appropriately on an implantable scaffold that both aligns and supports the viability of cell grafts is a prerequisite for an effective scaffold design to be used as part of a strategy for the treatment of SCI. Cell viability within scaffolds after implantation can be an issue as seen with poly-D lactide matrices plated with immature astrocytes.[34] We have used a PCL embossed, aligned micropattern scaffold containing pores and microgrooves plated with mixed dissociated spinal cord cells mimicking the CNS that will contact the scaffold after implantation, to investigate the effect of several polymers on these cells ability to survive and differentiate. We found that PLL-coated PCL was the optimal substrate to support myelination and inclusion of surface topography necessary for generating a future 3D design did not affect these properties. However, we also found that myelination in these cultures plated onto PCL is delayed compared to controls, due to differences in oligodendrocyte maturation. This suggests a substrate-specific effect of the PCL upon CNS cells within the culture. From astrocyte conditioning experiments (Fig. 7), the reduction in myelination is unlikely to be a direct, contact-mediated effect of PCL; it seems more likely that the PCL substrate alters the secretory profile of astrocytes.

Although myelinating cultures focus on *in vitro* interaction, they enable examination of many aspects of cell interactions that occur in the intact CNS, including cross talk between astrocytes, neurons, and multiple glia.[35] Importantly, these cultures allow the study of myelin sheath formation, rather than relying entirely on the expression of late myelin markers. Myelin ensheathment observed in these cultures is similar to myelination and sheath formation *in vivo*.[23–26] One important feature of the myelinating culture is ensuring that the neurite density is comparable between

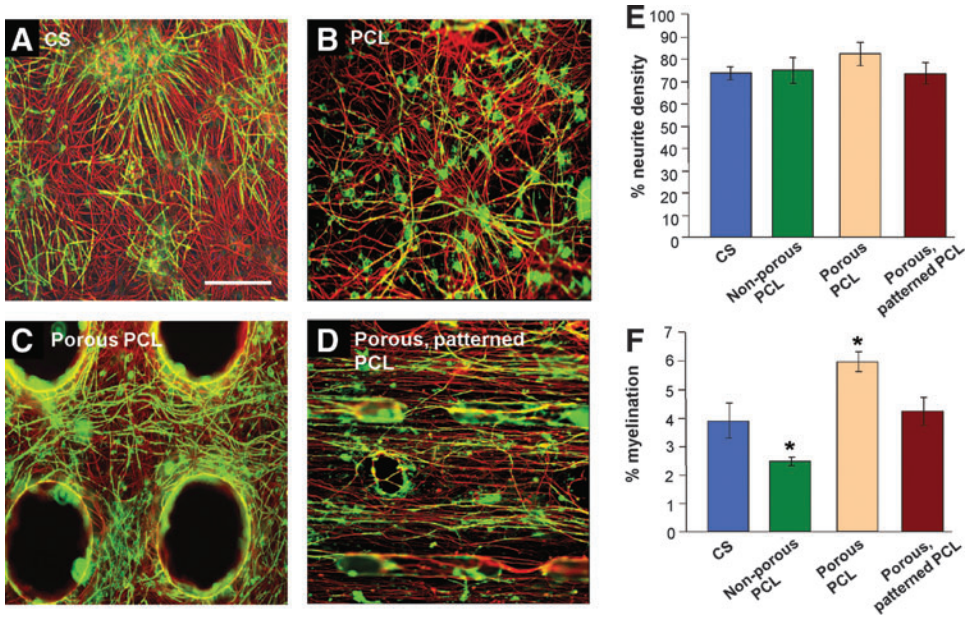

FIG. 6. Myelination on PCL membranes reaches control levels over extended culture time. Representative images of myelinating cultures on glass coverslips **(A)**, nonporous PCL **(B)**, porous PCL **(C)**, and porous, micropatterned PCL **(D)**, immunolabeled for SMI-31 (red), and PLP (green). Quantification of neurite density **(E)** showed levels were similar on all membranes tested. Quantification of myelination **(F)** demonstrates that myelination on the PCL membranes is comparable to that found on glass coverslip control ($n = 3$, t-test, Bonferroni corrected, $^*p < 0.05$). Scale bar: 200 μm. Color images available online at www.liebertpub.com/tea

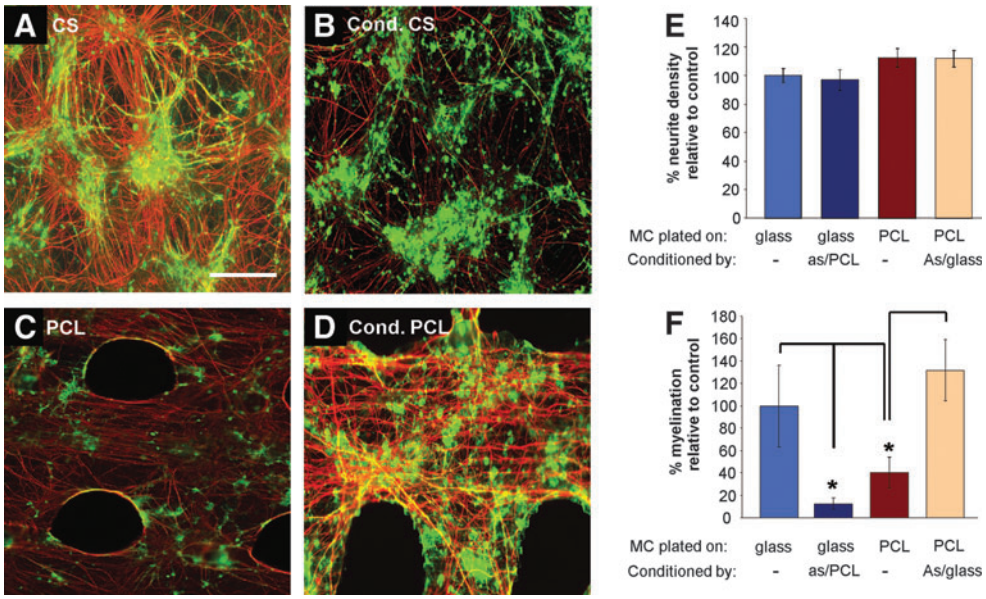

FIG. 7. Astrocytes plated on PCL delay myelination. Representative images of myelinating cultures plated on: glass coverslips **(A, B)** and PCL **(C, D)**, with the cultures undergoing conditioning by either astrocytes plated onto PCL **(B)**, or astrocytes plated onto coverslips **(D)**. Cultures were immunolabeled for SMI-31 (red) and PLP (green). Scale bar: 100 μm. Quantification of neurite density **(E)** showed that there were no significant differences for each substrate; however, quantification of myelination **(F)** demonstrated that cultures plated on PCL conditioned with astrocytes plated on glass coverslips **(D)** had levels of myelination comparable to cultures plated on glass coverslips. Conversely, myelinating cultures plated on glass coverslips and conditioned with astrocytes plated on PCL **(B)** displayed significantly lower levels of myelination compared to control cultures plated on glass coverslips (All $n = 3$, t-test, Bonferroni corrected, $^*p < 0.05$). Color images available online at www.liebertpub.com/tea

control and experimental cultures. A low neurite density suggests that viability may be compromised and the number of neurites available for myelination is decreased affecting the level of myelination calculated (less total neurites/myelin sheath would give a higher percentage of myelinated fibers). Despite comparable neurite densities between each of the polymers tested, a significantly reduced level of myelination was observed in the cultures at 28 DIV compared to control cultures plated on glass coverslips, suggesting that all the substrates affected myelination. With PLLA, PGLA, and polycarbonate, all of which have been considered as suitable potential candidates for transplantation into CNS injury,[36–40] this difference in supporting myelination highlights the importance of examining interactions of candidate substrates with CNS cells beyond just neurite outgrowth. PDMS, on the other hand, is not a biodegradable material, even though it is extensively used in biomedical engineering, incorporated into microscale devices and permanent implants.[40,41]

The molecular weight of the macromer units can have a significant effect on the final polymer interactions with CNS cells, with a lower molecular weight PCL being more supportive of myelination compared to the other polymers, including a higher molecular weight PCL. The influence of macromer weights on cells has been recognized in hydrogels,[41] although the lower molecular weight PCL was unsuitable for fabrication, as the PCL membrane degraded during the embossing procedure. Thus, high molecular weight PCL, which appeared to be the next best substrate, was selected as the candidate material for further development. Our results show that PCL appears to be a useful support for CNS cells as it not only allows their adhesion, survival, but also differentiation. Its potential use as a scaffold for cell transplantation has added support by its long degradation time.[23,42] The degradation of radioactive-tagged PCL transplanted subcutaneously into rats and followed over 3 years was very slow. Over the first 2 years it broke down into small molecular weight material by random, spontaneous hydrolysis, eventually the degraded material would be metabolized, although its overall shape still was recognizable (Sun *et al.* 2006). Thermoplastic forming similar to the manipulations needed to shape the scaffold presented here do not affect the degradation time as shown by Lam *et al.* (2008). As repair in the CNS is predicted to take a relatively long time, it is thought that a PCL scaffold would allow enough time for nerves and endogenous cells to regrow across the scaffold and become myelinated, and secrete the appropriate ECM to bridge the lesion, before the scaffold degrades.

Previous work using myelinating cultures has demonstrated that between 24–28 DIV was sufficient to assess myelination levels and was used in initial studies of the PCL scaffolds with topographical features important for the final design of a 3D scaffold for implantation *in vivo*.[21,31] However, the significantly lower level of myelination at 28 DIV across the PCL substrates irrespective of topographical features, compared with control cultures suggested a dominant, substrate-specific effect. This effect of PCL on myelination was not due to cytotoxicity due to impurities in the PCL or degradation products[43] or the higher hydrophobicity of PCL when compared to glass coverslips. ECM molecules (collagen, fibronectin, and laminin), traditionally used in neuronal cultures to promote survival and neurite outgrowth,[44–47] did not enhance myelination. The myelinating cultures plated onto PCL coated with laminin displayed significantly lower neurite outgrowth than the other conditions, even though the astrocyte monolayer, critical for neurite survival in this system, was intact. The possibility exists that a more specific treatment regime is required for the ECM molecules to promote myelination. However, a similar reduction in myelination was observed when astrocytes were plated on glass coverslips coated with the ECM molecule tenascin C.[30] A subsequent microarray study of astrocytes plated either on tenascin C or PLL identified the chemokine CXCL10 as a factor secreted by astrocytes, which inhibited myelination. Thus, this data further supports the concept that modification of the astrocyte phenotype by ECM molecules influences glial/axonal interactions.[30,48]

To dissect how myelination was perturbed on PCL, we observed oligodendrocyte differentiation from progenitor cell to maturity using a panel of markers. There were a greater number of early OPCs, immature oligodendrocytes, and premyelinating oligodendrocytes, but less mature oligodendrocytes. These data coupled with decreased myelination and apparent ensheathment with anti-PLP and the recovery of myelination to control levels at 46 DIV suggested that although PCL delayed oligodendrocyte differentiation, this was not detrimental to myelination.

Previously, we and others have shown the astrocyte reactive status or phenotype can influence myelination[30,48–51] within myelinating cultures. Astrocytes made quiescent by plating on tenascin C[52] reduced the percentage of myelination in cultures plated onto them. Since quiescent astrocytes (plated on tenascin C) were shown to secrete an inhibitory factor for myelination, CXCL10, astrocytes on PCL could conceivably secrete factors that have a similar effect.[30] However, the effect is also reversible as seen by the enhancement of myelination following exposure to astrocyte-conditioned media from astrocytes grown on glass coverslips. Thus, we suggest that astrocytes plated on PCL initially have a phenotype less supportive for myelination; however, they adopt a phenotype conducive of myelination over time. This delay of myelination mediated by the influence of PCL on the astrocytes can be overcome by factors secreted by astrocytes plated on coverslips. These astrocytes appear to secrete factors that either directly promote myelination or counteract the delaying effect of PCL on myelination. These findings suggest that the effects of PCL on myelination are, at least, in part, an indirect one, by proxy of the astrocyte monolayer, altering their secretory profile.

Conclusion

In this study, we have confirmed that a PCL scaffold with topography is a suitable substrate for the design of a 3D scaffold for inplantation into animal models of SCI. Furthermore, myelination was delayed on the PCL substrate by factors secreted by astrocytes. However, this short delay was not a caveat for the use of PCL in the design of a 3D scaffold for transplantation into the injured CNS.

Acknowledgments

The work described in the article was funded by the Biotechnology and Biological Sciences Research Council

(BB/G004706/1) (BBSRC, PD, ST); Lord Kelvin and Adam Smith PhD studentship (RL) and NC3Rs (SDB).

Disclosure Statement

No competing financial interests exist for all authors.

References

1. Fitch, M.T., and Silver, J. CNS injury, glial scars, and inflammation: inhibitory extracellular matrices and regeneration failure. Exp Neurol **209,** 294, 2008.
2. Fawcett, J.W., and Asher, R.A. The glial scar and central nervous system repair. Brain Res Bull **49,** 377, 1999.
3. Barnett, S.C., and Riddell, J.S. Olfactory ensheathing cell transplantation as a strategy for spinal cord repair—what can it achieve? Nat Clin Pract Neurol **3,** 152, 2007.
4. Toft, A., Scott, D.T., Barnett, S.C., and Riddell, J.S. Electrophysiological evidence that olfactory cell transplants improve function after spinal cord injury. Brain **130,** 970, 2007.
5. Nomura, H. Tator, C.H., and Stoichet, M.S. Bioengineered strategies for spinal cord repair. J Neurotrauma **23,** 495, 2006.
6. Fawcett, J.W. Bridging spinal cord injuries. J Biol **7,** 25, 2008.
7. Madigan, N.N., McMahon, S., O'Brien, T., Yaszemski, M.J., and Windebank, J. Current tissue engineering and novel therapeutic approaches to axonal regeneration following spinal cord injury using polymer scaffolds. Respir Physiol Neurobiol **169,** 183, 2009.
8. Kubinová, S., and Syková, E. Nanotechnology for treatment of stroke and spinal cord injury. Nanomedicine **5,** 99, 2010.
9. Straley, K.S., Foo, C.W., and Heilshorn, S.C. Biomaterial design strategies for the treatment of spinal cord injuries. J Neurotrauma **27,** 1, 2010.
10. Thouas, G.A., Contreras, K.G., Bernard, C.C., Sun, G.Z., Tsang, K, Zhou, K, *et al.* Biomaterials for spinal cord regeneration: outgrowth of presumptive neuronal precursors on electrospun poly(epsilon)-caprolactone scaffolds microlayered with alternating polyelectrolytes. Conf Proc IEEE Eng Med Biol Soc **2008,** 1825, 2008.
11. Hurtado, A., Cregg, J.M., Wang, H.B., Wendell, D.F., Oudega, M, Gilbert, R.J., *et al.* Robust CNS regeneration after complete spinal cord transection using aligned poly-L-lactic acid microfibers. Biomaterials **32,** 6068, 2011.
12. Luo, Y., and Shoichet, M.S. A photolabile hydrogel for guided three-dimensional cell growth and migration. Nat Mater **3,** 249, 2004.
13. Gelain, F., Panseri, S., Antonini, S., Cunha, C., Donega, M., Lowery, J., *et al.* Transplantation of nanostructured composite scaffolds results in the regeneration of chronically injured spinal cords. ACS Nano **5,** 27, 2011.
14. Thuaksuban, N., Nuntanaranont, T., Pattanachot, W., Suttapreyasri, S., and Cheung, L.K. Biodegradable polycaprolactone-chitosan three-dimensional scaffolds fabricated by melt stretching and multilayer deposition for bone tissue engineering: assessment of the physical properties and cellular response. Biomed Mater **6,** 015009, 2011.
15. Zhong, X., Ji, C., Chan, A.K., Kazarian, S.G., Ruys, A., and Dehghani, F. Fabrication of chitosan/poly(epsilon-caprolactone) composite hydrogels for tissue engineering applications. J Mater Sci Mater Med **22,** 279, 2011.
16. Sahni, V., and Kessler, J.A. Stem cell therapies ofr spinal cord injury. Nat Rev Neurol **6,** 363, 2010.
17. Baptiste, D.C., and Fehlings, M.G. Update on the treatment of spinal cord inury. Prog Brain Res **161,** 217, 2007.
18. Radtke, C., Sasaki, M., Lankford, KL, Vogt, P.M., and Kocsis, J.D. Potential of olfactory ensheathing cells for cell-based therapy in spinal cord injury. J Rehabil Res Dev **45,** 141, 2008.
19. Hwang, D.H., Kim, H.M., Kang, Y.M., Joo, I.S., Cho, C.S., Yoon, B.W., *et al.* Combination of multifaceted strategies to maximize the therapeutic benefits of neural stem cell transplantation for spinal cord repair. Cell Transplant **20,** 1361, 2011.
20. Horne, M.K., Nisbet, D.R., Forsythe, J.S., and Parish, C.L. Three-dimensional nanofibrous scaffolds incorporating immobilized BDNF promote proliferation and differentiation of cortical neural stem cells. Stem Cells Dev **19,** 843, 2010.
21. Sørensen, A., Alekseeva, T., Katechia, K., Robertson, M., Riehle, M.O., and Barnett, S.C. Long-term neurite orientation on astrocyte monolayers aligned by microtopography. Biomaterials **28,** 5498, 2007.
22. Seunarine, K., Meredith, D.O., Riehle, M.O., Wilkinson, C.D.W., and Gadegaard, N. Biodegradable polymer tubes with lithographically controlled 3D micro- and nanotopography, Microelect Eng **85,** 350, 2008.
23. Sun, T., Donoghue, P.S., Higginson, J.R., Gadegaard, N., Barnett, S.C., and Riehle, M.O. The interactions of astrocytes and fibroblasts with defined pore structures in static and perfusion cultures. Biomaterials **32,** 2021, 2011.
24. Sørensen, A., Moffat, K., Thomson, C., and Barnett, S.C. Astrocytes, but not olfactory ensheathing cells or Schwann cells, promote myelination of CNS axons *in vitro*. Glia **56,** 750, 2008.
25. Thomson, C.E., McCulloch, M., Sorenson, A., Barnett, S.C., Seed, B.V., Griffiths, I.R., *et al.* Myelinated, synapsing cultures of murine spinal cord—validation as an *in vitro* model of the central nervous system. Eur J Neurosci **28,** 1518, 2008.
26. Ioannidou, K., Anderson, K.I., Strachan, D., Edgar, J.M., and Barnett, S.C. Time-lapse imaging of the dynamics of CNS glial-axonal interactions *in vitro* and *ex vivo*. PLoS One **7,** 1, 2012.
27. Silva, N.A., Salgado, A.J., Sousa, R.A., Oliveira, J.T., Pedro, A.J., Leite-Almeida, H., *et al.* Development and characterization of a novel hybrid tissue engineering-based scaffold for spinal cord injury repair. Tissue Eng Part A **16,** 45, 2010;
28. Yamamura, T., Konola, J.T., Wekerle, H., and Lees, M.B. Monoclonal antibodies against myelin proteolipid protein: identification and characterization of two major determinants. J Neurochem **57,** 1671, 1991.
29. Sommer, I., and Schachner, M. Monoclonal antibodies (O1 to O4) to oligodendrocyte cell surfaces: an immunocytological study in the central nervous system. Dev Biol **83,** 311, 1981.
30. Nash, B., Thomson, C.E., Linington, C., Arthur, A.T., McClure, J.D., McBride, M.W., and Barnett, S.C. Functional duality of astrocytes in myelination. J Neurosci **31,** 13028, 2011.
31. Sun, T., Donoghue, P.S., Higginson, J.R., Gadegaard, N., Barnett, S.C., and Riehle, M.O. A miniaturized bioreactor system for the evaluation of cell interaction with designed substrates in perfusion culture. J Tissue Eng Regen Med 2011. [Epub ahead of print]; DOI: 10.1002/term.510.
32. Colognato, H., Galvin, J., Wang, Z., Relucio, J., Nguyen, T., Harrison, D., Yurchenco, P.D., and Ffrench-Constant, C. Identification of dystroglycan as a second laminin receptor in oligodendrocytes, with a role in myelination. Development **134,** 1723, 2007.
33. Chun, S.J., Rasband, M.N., Sidman, R.L., Habib, A.A., and Vartanian, T. Integrin-linked kinase is required for

laminin-2-induced oligodendrocyte cell spreading and CNS myelination. J Cell Biol **163,** 397, 2003.
34. Deumens, R., Koopmans, G.C., Honig, W.M., Maquet, V., Jérôme, R., Steinbusch, H.W., and Joosten, E.A. Limitations in transplantation of astroglia-biomatrix bridges to stimulate corticospinal axon regrowth across large spinal lesion gaps. Neurosci Lett **400,** 208, 2006.
35. Boomkamp, S.D., Riehle, M.O., Wood, J., Olson, M.F., and Barnett, S.C. The Development of a rat in vitro model of spinal cord injury demonstrating the additive effects of Rho and ROCK inhibitors on neurite outgrowth and myelination. Glia **60,** 441, 2012
36. Wang, H.B., Mullins, M.E., Cregg, J.M., Hurtado, A., Oudega, M., Trombley, M.T., *et al.* Creation of highly aligned electrospun poly-L-lactic acid fibers for nerve regeneration applications. J Neural Eng **6,** 016001, 2009.
37. Wang, Y., Wei, Y.T., Zu, Z.H., Ju, R.K., Guo, M.Y., Wang, X.M., *et al.* Combination of hyaluronic acid hydrogel scaffold and PLGA microspheres for supporting survival of neural stem cells. Pharm Res **28,** 1406, 2011.
38. Montgomery, C.T., and Robson, J.A. Implants of cultured Schwann cells support axonal growth in the central nervous system of adult rats. Exp Neurol **122,** 107, 1993.
39. Hassler, C., Boretius, T., and Stieglitz, T. Polymers for neural implants. J Polym Sci Part B: Polym Phys **49,** 18, 2011.
40. McClain, M.A., Clements, I.P., Shafer, R.H., Bellamkonda, R.V., LaPlaca, M.C., and Allen, M.G. Highly compliant, microcable neuroelectrodes fabricated from thin-film gold and PDMS. Biomed Microdevices **13,** 361, 2011,
41. Lampe, K.J., Mooney, R.G., Bjugstad, K.B., and Mahoney, M.J. Effect of macromer weight percent on neural cell growth in 2D and 3D nondegradable PEG hydrogel culture. J Biomed Mater Res A **94,** 1162, 2010.
42. Lam, C.X., Savalani, M.M., Teoh, S.H., and Hutmacher, D.W. Dynamics of *in vitro* polymer degradation of polycaprolactone-based scaffolds: accelerated versus simulated physiological conditions. Biomed Mater **3,** 034108, 2008.
43. McDonald, G.R., Hudson, A.L., Dunn, S.M., You, H., Baker, G.B., Whittal, R.M., *et al.* Bioactive contaminants leach from disposable laboratory plasticware. Science **322,** 917, 2008.
44. Oztürk, G., Sekeroglu, M.R., Erdoğan, E., and Oztürk, M. The effect of non-enzymatic glycation of extracellular matrix proteins on axonal regeneration *in vitro.* Acta Neuropathol **112,** 627, 2006.
45. Zhang, Z., Yoo, R., Wells, M., Beebe, T.P. Jr, Biran R., and Tresco, P. Neurite outgrowth on well-characterized surfaces: preparation and characterization of chemically and spatially controlled fibronectin and RGD substrates with good bioactivity. Biomaterials **26,** 47, 2005.
46. Mukhatyar, V.J., Salmeron-Sanchez, M., Rudra, S., Mukhopadaya, S., Barker, T.H., García, A.J., and Bellamkonda, R.V. Role of fibronectin in topographical guidance of neurite extension on electrospun fibers. Biomaterials **32,** 3958, 2011.
47. Zander, N.E., Orlicki, J.A., Rawlett, A.M., and Beebe, T.P. Jr. Surface-modified nanofibrous biomaterial bridge for the enhancement and control of neurite outgrowth. Biointerphases **5,** 149, 2010.
48. Sofroniew, M.V., and Vinters, H.V. Astrocytes: biology and pathology. Acta Neuropathol **119,** 7, 2010.
49. Stankoff, B., Aigrot, M.S., Noël, F., Wattilliaux, A., Zalc, B., and Lubetzki, C. Ciliary neurotrophic factor (CNTF) enhances myelin formation: a novel role for CNTF and CNTF-related molecules. J Neurosci **22,** 9221, 2002.
50. Williams, A., Piaton, G., and Lubetzki, C. Astrocytes—friends or foes in multiple sclerosis? Glia **55,** 1300, 2007.
51. Schaub, N.J., and Gilbert, R.J. Controlled release of 6-aminonicotinamide from aligned, electrospun fibers alters astrocyte metabolism and dorsal root ganglia neurite outgrowth. J Neural Eng **8,** 046026, 2011.
52. Holley, J.E., Gveric, D., Whatmore, J.L., and Gutowski, N.J. Tenascin C induces a quiescent phenotype in cultured adult human astrocytes. Glia **52,** 53, 2005.

Address correspondence to:
Susan C. Barnett, BSc, PhD
Institute of Infection
Immunity and Inflammation
College of Medical, Veterinary and Life Sciences
Room B3/29
University of Glasgow
120 University Place
Glasgow G12 8TA
United Kingdom

E-mail: susan.barnett@glasgow.ac.uk

Received: June 18, 2012
Accepted: September 14, 2012
Online Publication Date: November 29, 2012